Sustainable and Surfactant-Free Synthesis of Negatively Charged Acrylamide Nanogels for Biomedical Applications

Davide Mazzali[a], Gabriela Rath[a], Alexander Röntgen[b], Vaidehi Roy Chowdhury[b], Michele Vendruscolo[b], Marina Resmini[a*]

[a] Department of Chemistry, SPCS, Queen Mary University of London, London E1 4NS, UK; [b] Centre for Misfolding Diseases, Yusuf Hamied Department of Chemistry, University of Cambridge, Cambridge CB2 1EW, UK.

Correspondence: m.resmini@qmul.ac.uk (M.R.)

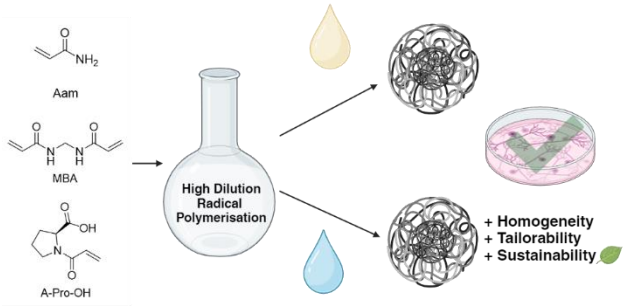

Abstract

Nanogels offer unique advantages, like high surface-to-volume ratio, scalable synthetic methods and easily tailored formulations, that allow to control size and introduce stimuli-responsive properties. Their potential for drug delivery is significant due to their biocompatibility, high drug loading capacity, and controlled and sustained drug release. However, the development of greener and sustainable processes, in particular the replacement of organic solvents with water, is essential for large-scale applications. To address this problem, we report the synthesis in water of covalently crosslinked acrylamide-based nanogels, both neutral and negatively charged, with varying amounts of acryloyl-L-proline, using a high-dilution radical polymerization technique without the need for surfactants. The use of a water-based synthesis allowed to obtain nanogels with high monomer conversions and chemical yields, as well as lower polydispersity and smaller particle sizes for

the negatively charged nanogels, compared to the same formulation prepared in organic solvents. This approach provides a more efficient synthetic methodology, with reduced loss of starting materials, higher potential for scalability and lower costs. The suitability of these nanogels for biomedical applications was supported by cytotoxicity studies showing no significant reduction in viability on a human neuroblastoma cell line.

1.0 Introduction

Innovative drug delivery systems are key in drug discovery and development as they enable the effective administration of therapeutic agents. Advances in the field of nanomaterials are contributing to address some of the challenges in drug delivery, such as the off-target toxicity, low loading capacity, and poor solubility of active molecules[1-3], with controlled release[4,5] and permeation through biological barriers[6] playing important roles. Among the systems being investigated are liposomes[7], polymeric nanoparticles (NPs)[8], micelles[9] and covalently crosslinked nanogels (NGs)[10], with the latter offering great potential[10]. NGs are characterized by small size (10 – 100 nm) and high drug loading capacity, while their formulation can be easily tailored to introduce stimuli-responsiveness to triggers such as infrared radiation[11], oxidation[12], temperature[13] and pH [14,15], an attractive feature for drug delivery applications[16-19].

The most common synthetic strategy for the preparation of NGs is radical polymerisation (RP)[20], either controlled[21-23] or free, either in heterogeneous or homogeneous phase. For all methods the control of the molecular weight is a priority, given its link to the properties of the isolated polymers[24]. Heterogeneous polymerisation techniques such as (inverse) emulsion/microemulsion/miniemulsion[25-27] or precipitation/dispersion[28] require surfactants to stabilise the growing polymeric chains and control the final particle size. The use of surfactants and emulsifiers, although advantageous, does require additional purification steps that can effect the drug loading as well as stability, while raising potential issues of toxicity *in vivo*[29]. High dilution radical polymerisation (HDRP) is a homogeneous polymerisation method that

does not require surfactants to obtain colloidally stable nanogels, and uses monomer concentrations to avoid macrogelation while controlling polymer weight[30]. HDRP can be optimised to lead high monomer conversions and yields, good control of particle size, and easy tailoring of the formulation with the addition of different functional monomers and crosslinkers.

We used HDRP in organic solvents for the synthesis of NGs for applications in catalysis[31], sensing[32] and drug delivery[33], focusing on the relationship between formulation and properties, their interaction with biomolecules *in vitro*[34], and the effect of different synthetic procedures[35]. As interest towards NGs continues to grow, especially in the biomedical field, issues around the use of organic solvents and sustainability of the process are becoming prominent. Studies of the effects of changing the solvent system include the synthesis of core-shell nano/microgels with polyethylene glycol chains using surfactant free emulsion polymerization in water[36], the impact of changing water-to-ethanol ratio in a cosolvent system[37], using biobased synthesis-solvents[38], effect of solvents on the swelling ability of bulk hydrogels[39] .

Although HDRP has been extensively employed for the synthesis of NGs in organic solvents[40-43], the use of water for a more sustainable and scalable approach has not been widely investigated. In this work, we report the green and surfactant-free synthesis in water and characterization of acrylamide-based NGs, covalently cross-linked (XL) with 20 molar% of *N,N'*-methylenebisacrylamide (MBA), neutral or negatively charged by the addition of varying amounts of the negatively charged acryloyl-*L*-proline (A-Pro-OH). Monomer conversions were determined by proton nuclear magnetic resonance (^{1}H-NMR) spectroscopy, while size, polydispersity, and surface charge were quantified using dynamic light scattering (DLS). All data were compared to the same formulations synthesized in DMSO to evaluate the effects of changing solvent on properties and morphology. The effects of changing solvent on the

cytotoxicity of NGs was also evaluated in SH-SY5Y (human neuroblastoma) cells, given the potential applications of NGs for drug delivery.

2.0 Materials and Methods

2.1 Materials

N,N'-methylenebisacrylamide (MBA, 99%), acrylamide (Aam, 98%), 1,2,4,5-tetramethylbenzene (TMB, 98%), *N,N,N′,N′*-tetramethylethylenediamine (TEMED, 99%), potassium persulfate (KPS, ≥ 99.0%), sodium phosphate dibasic heptahydrate, and sodium phosphate monobasic heptahydrate were purchased from Sigma-Aldrich UK and employed as received. 2,2′-Azobis(2-methylpropionitrile) (AIBN, 98%) was purchased from Sigma-Aldrich UK and used after recrystallization in methanol. Dry dimethyl sulfoxide (DMSO, 99%) was purchased from Goss Scientific UK, and deuterated dimethyl sulfoxide (DMSO-d_6, 99%) was purchased from Cambridge Isotope Laboratories. Acryloyl-*L*-proline (A-Pro-OH) was synthesised using a previously reported procedure[44]. Dialysis membranes (molecular weight cut-off 3.5 kDa) were purchased from Medicell International Ltd. Poly(ethersulfone) (PES) syringe filters with pore sizes of 0.2 µm were obtained from FisherScientific (Loughborough, UK). The 3-(4,5-dimethylthiazol-2-yl)-2,5-diphenyltetrazolium bromide (MTT) Assay Kit was purchased from Abcam UK, and Dulbecco's Modified Eagle Medium (DMEM/F-12), GlutaMAX™ supplement, RPMI cell medium 1640, fetal bovine serum (FBS), trypsin-EDTA (0.25%), and Dulbecco's phosphate buffered saline (DPBS - $MgCl_2$ - $CaCl_2$) were purchased from ThermoFisher Scientific.

2.2 Synthesis of NGs in DMSO

For a standard preparation containing Aam and MBA in the ratio 80:20 (molar%), the calculated quantities of Aam (back-bone monomer), MBA (cross-linker), and initiator (AIBN) were weighed according to each formulation and dissolved in dry DMSO in a round bottom flask (RBF). The volume of DMSO was calculated to obtain a 1% (*w/w*) final monomer

concentration. AIBN (initiator) was added to the RBF at a concentration of 1% of the total moles of double bonds in the reaction mixture, after which the RBF was sealed and purged with nitrogen. The vessel was then placed in an oil bath at 70 °C for 24 h. 100 µL samples to quantify monomer conversions were taken at the start (t = 0 h) and at the end (t = 24 h) of the reaction.

2.3 Synthesis of NGs in water

The synthesis of NGs in water followed the same procedure described in 2.2, with the moles of KPS and TEMED calculated to be 1% and 5% of the total moles of double bonds, respectively. To prevent the reaction from starting prematurely, these were weighed and solubilized in a separate RBF, which was also purged with nitrogen. The concentration of the initiators stock solution was determined so that 1 mL of solution would be added to the reaction mixture to bring its final concentration to 1% *(w/w)* (comparable to the DMSO synthesis). After adding the initiator solution, the reaction mixture was placed in a pre-heated oil bath at 30 °C. 100 µL samples to quantify monomer conversions were taken at the start (t = 0 h) and at the end (t = 24 h) of the reaction.

2.4. Purification and isolation of NGs

After polymerization, NGs were dialyzed against deionized water for at least 48 h, changing water every 8 h. Purified NGs were freeze-dried for at least 2 days, and stored at room temperature (RT) until use.

2.5 Monomer conversion via ^{1}H-NMR spectroscopy

Monomer conversion was evaluated by ^{1}H-NMR spectroscopy for each formulation at t = 0 h and t = 24 h. TMB was used as the internal standard (IS) at a final concentration of 20 mg/mL in DMSO-d_6, with total volumes yielding 500 µL. ^{1}H-NMR spectra were acquired in the solvent suppression mode at 298 K using a Bruker AVIII400 spectrometer (400 MHz). Spectra were processed with TopSpin software (version 4.2.0, Bruker) to

quantify the signal of each monomer at t=0 h and t=24 h (Aam at δ = 6.04 ppm, A-Pro-OH at δ = 6.61 ppm and MBA at δ = 5.63 ppm) by integrating it against the peak of the arylic protons of the IS (δ = 6.87 ppm).

2.6 Particle size measurement by dynamic light scattering

NGs samples for DLS were prepared by dispersing about 3 mg of dry polymer in phosphate buffer (PB) 10 mM pH 7.4 at a final concentration of 1 mg/mL. The solution was sonicated for 10 min and filtered using a 0.2 µm PES filter directly to a disposable plastic pre-cleaned cuvette (Fisher Scientific, Leicestershire, UK, catalogue no.15520814) to minimize dust contamination. Samples were analyzed in triplicate at 25°C using a Malvern Zetasizer Ultra. Backscatter (173°) angle mode was used to determine size distribution and polydispersity index (PDI) for each sample. Data were processed using software ZX Xplorer (v2.2.0.147, Malvern Panalytical Ltd., Malvern, UK) and plotted as mean values ± standard deviation (SD), using GraphPad Prism 10.0.0.

2.7 ζ-potential analysis

NGs samples for DLS were prepared by dispersing about 3 mg of dry polymer in phosphate buffer (PB) 10 mM pH 7.4 at a final concentration of 1 mg/mL. The solution was sonicated for 10 min and filtered using a PES filter 0.2 µm directly to a disposable folded capillary cell (1080, Malvern Panalytical Ltd., Malvern, UK), To minimize dust contamination, the capillary cell was flushed with compressed air and washed with PB immediately before sample were transferred. Samples were analyzed in triplicate at 25 °C using a Malvern Zetasizer Ultra.

2.8 Acute cytotoxicity studies: SH-SY5Y cells

Human SH-SY5Y neuroblastoma cells were cultured in DMEM/F-12, GlutaMAX™ supplemented with 10% (v/v) FBS on 75 cm^2 treated polystyrene flasks (Greiner Bio-One). Cells were grown at 37 °C in a 5% CO_2-humified atmosphere and split at 80%

confluency. Cell viability was measured using the MTT assay. Cells were seeded on 96-well plates (Greiner Bio-One) at a density of 10,000 cells/well in 100 µL cell medium. After incubation for 24 h at 37 °C, the medium was replaced either with fresh medium (medium control), 10% (*v/v*) ultrapure water in fresh medium (vehicle control), or nanoparticles in 10% (*v/v*) ultrapure water in fresh medium. Cells were treated in quintuplicates and incubated for another 24 h at 37 °C. After that, the medium was discarded, and cells were incubated with 0.5 mg/mL MTT in RPMI medium for 4 h at 37 °C. The solution was discarded, and the formazan product was solubilized by incubation in cell lysis buffer (100 µL per well) at 500 rpm and 37 °C for 15 min on a PHMP Grant-Bio Thermoshaker. Absorbance at λ = 570 nm was measured on a CLARIOStar plate reader (BMG Labtech), and cell viability was normalized to the medium control.

2.9 Transmission electron microscopy

Nanogels were imaged using transmission electron microscopy, both in dry state and in cryogenic mode. Briefly, 8 µL of each reconstituted solution were deposited on a copper grid (Agar Scientific, UK), blotted and stained with a 1% solution of uranyl acetate in water. For cryogenic-TEM, 4 µL of each solution were deposited on a copper grid (Agar Scientific, UK), blotted and immediately frozen by plunging in liquid ethane bath. The samples were imaged using a JEM-F200 microscope (200 kV, JEOL Ltd., Tokyo, Japan). ImageJ (v.1.54) was used to analyze and measure the size of the particles.

2.10 Data Analysis

Data visualization and analysis (monomer conversion, chemical yield, DLS measurements, and cell viability) were performed using GraphPad Prism 10.0.0, plotting mean values ± SD, unless otherwise specified. Data were analyzed for normal distribution using the Shapiro-Wilk test. Two-way ANOVA with Šídák's multiple comparisons test was used to analyze the monomer conversion and chemical yield,

while one-way ANOVA was used for DLS data. Multiple comparison Student's *t*-test was used to analyze polydispersity values. Mann-Whitney's test was used to analyze size values obtained from TEM imaging.

3. Results and Discussion

3.1 Synthesis and characterization of NGs: monomer conversion and chemical yield

A small library of ten NGs was synthesized via HDRP following our previously reported protocol[35] using DMSO or water as the solvent (**Table 1**) and without the addition of any surfactants. Aam (**Figure 1**) was chosen as the backbone monomer, given its solubility in both solvent systems (DMSO and water). The cross-linker (MBA) content was fixed at 20 molar%, as this amount was found to be optimal for drug loading[33] and could provide a good balance between flexibility of the matrix and the three-dimensional structure of the NG. A-Pro-OH was added as functional monomer designed to impart a negative charge to the NGs, introducing a potentially pH-responsive trigger.

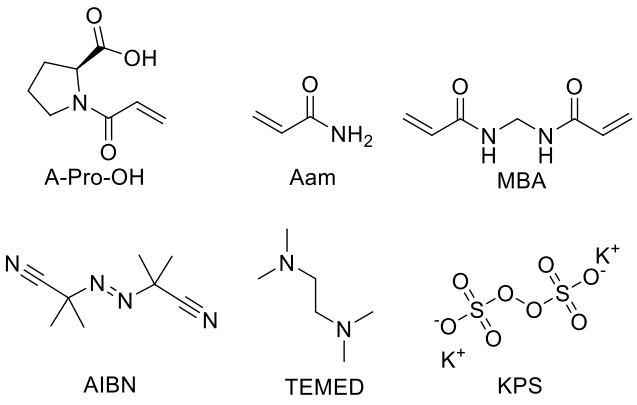

Figure 1. Chemical structures of monomers and cross-linker (MBA) used in this study.

The A-Pro-OH monomer content in the formulations was varied between 2.5 and 15 molar% to evaluate the impact of the negative charge on the morphology and the cytotoxicity of the NGs. For all preparations the total monomer concentration (C_m) was kept to 1% *(w/w)*, using AIBN as initiator for the NGs prepared in DMSO, while KPS/TEMED was used

for the formulations synthesized in water, given AIBN's limited solubility in this solvent[45]. The preparation of NGs in both systems was justified by the objective of evaluating how the change to a more sustainable and greener solvent could impact the NG morphology and properties. All the formulations were prepared in triplicates to ensure the reproducibility of the synthetic procedure.

Table 1. Chemical composition of the nanogels synthesised for this study. All the preparations were prepared in triplicate.

Formulation	Synthetic solvent	Aam (% mol/mol)	MBA (% mol/mol)	A-Pro-OH (% mol/mol)
NG1	DMSO	80	20	0
NG2		77.5		2.5
NG3		75		5
NG4		70		10
NG5		65		15
NG6	WATER	80	20	0
NG7		77.5		2.5
NG8		75		5
NG9		70		10
NG10		65		15

Given the random nature of radical polymerization, any evaluation of solvent effect on the NGs required evidence of consistency between formulation and final chemical composition of the isolated polymers. For this reason, monomer conversions (determined by ^{1}H-NMR, **Figure S1**) and chemical yields were quantified (**Figure 2**).

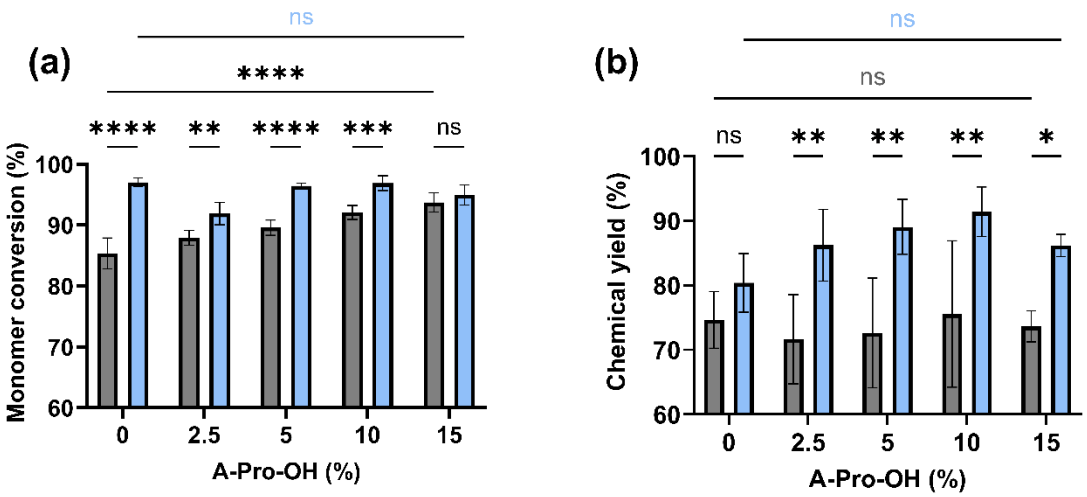

Figure 2. (a,b) Total monomer conversion (a) and chemical yields (CY) (b) for nanogels synthesised in DMSO (grey) and water (light blue). Data are presented as mean values ± SD (n=3), ** p < 0.01, *** p < 0.001, **** p < 0.0001.

The synthetic procedure yielded high total monomer conversions for all the formulations tested (**Figure 2a**, MC_t > 80%). However, the neutral NG synthesized in water had a significantly ($p < 0.001$) higher MC_t than the one obtained in DMSO, as a result of the different reactivity of Aam in the alternative solvent systems[46,47]. Aam is fully solvated and protonated in water, which reduces the rate of bimolecular chain termination (via electrostatic interactions) and destabilizes the unpaired electron, leading to a higher reactivity. In contrast, Aam exists mainly as dimer/trimer in DMSO due to its reduced ability to form H-bonds with the solvent, which leads to a slower propagation step of the polymerization[48]. This difference was confirmed by the evaluation of the monomer conversions for the individual components (MC_s), showing how the reaction for Aam never exceeded 80%. (**Table S1**, ESI). When the negatively charged functional monomer A-Pro-OH was introduced in the formulation, the MC_t for all DMSO NGs increased (**Figure 2a**), even at the lowest concentration of 2.5 molar%. This result is not surprising, given that the A-Pro-OH monomer was previously shown to have a higher reactivity than Aam in DMSO[49]. This effect increased steadily with increasing A-Pro-OH molar content, up to 15 molar%, providing evidence of the positive impact on MC_t of the functional monomer in the formulation. At the

highest A-Pro-OH concentration, no significant difference ($p = 0.30$) was observed in MC_t between formulations prepared in DMSO and water. In the case of NGs synthesized in water, the addition of the negatively charged functional monomer did not impact the formulations, with no significant difference ($p > 0.01$) in MC_t between neutral and negatively charged NGs.

The change of the polymerization solvent from DMSO to water had a remarkable effect on the chemical yields (**Figure 2b**). As opposed to the MC_t data, the choice of solvent did not significantly ($p = 0.26$) impact the chemical yield of neutral NGs, however when the functional monomer A-Pro-OH was added the chemical yields for the water NGs were consistently much higher than for DMSO NGs. This is particularly interesting given that all the polymerizations were carried out at the same total monomer concentration (1%). At the lowest concentration of A-Pro-OH (2.5 molar%) there was already a significant difference ($p < 0.01$) in chemical yields obtained between the same formulation in water *vs* DMSO, due to the lower reactivity of Aam in the latter[48]. This effect became more significant ($p < 0.01$) when higher amounts of functional monomer were added to the formulation (up to 15 molar%). However, the chemical yields of the negatively charged NGs prepared in water were not significantly impacted by the increased amount of functional monomer. The differences observed between water and DMSO could be the result of variations in particles size but also polydispersity of the preparations, hence requiring further characterization.

3.2 D_h and ζ-potential analysis via DLS

DLS measurements were carried out to analyze the particle sizes with NG solutions in phosphate buffer (10 mM pH 7.4) forming stable colloidal solutions. The measurements (**Figure 3a**) showed that NGs synthesized in DMSO resulted in particles with hydrodynamic diameter (D_h) less than 10 nm (**Figure S2**), for both neutral and negatively charged particles, which is consistent with previously reported data[50]. Polymerization in DMSO with CM_t = 1% *(w/w)* is affected by the solvent limiting the reactivity of Aam[48], stabilizing the growing polymeric chains and leading to smaller particles. In addition, when the functional monomer A-Pro-OH

was introduced in the formulation, the size was not impacted, regardless of its concentration. All the nanogels showed an average D_h of around 10 nm

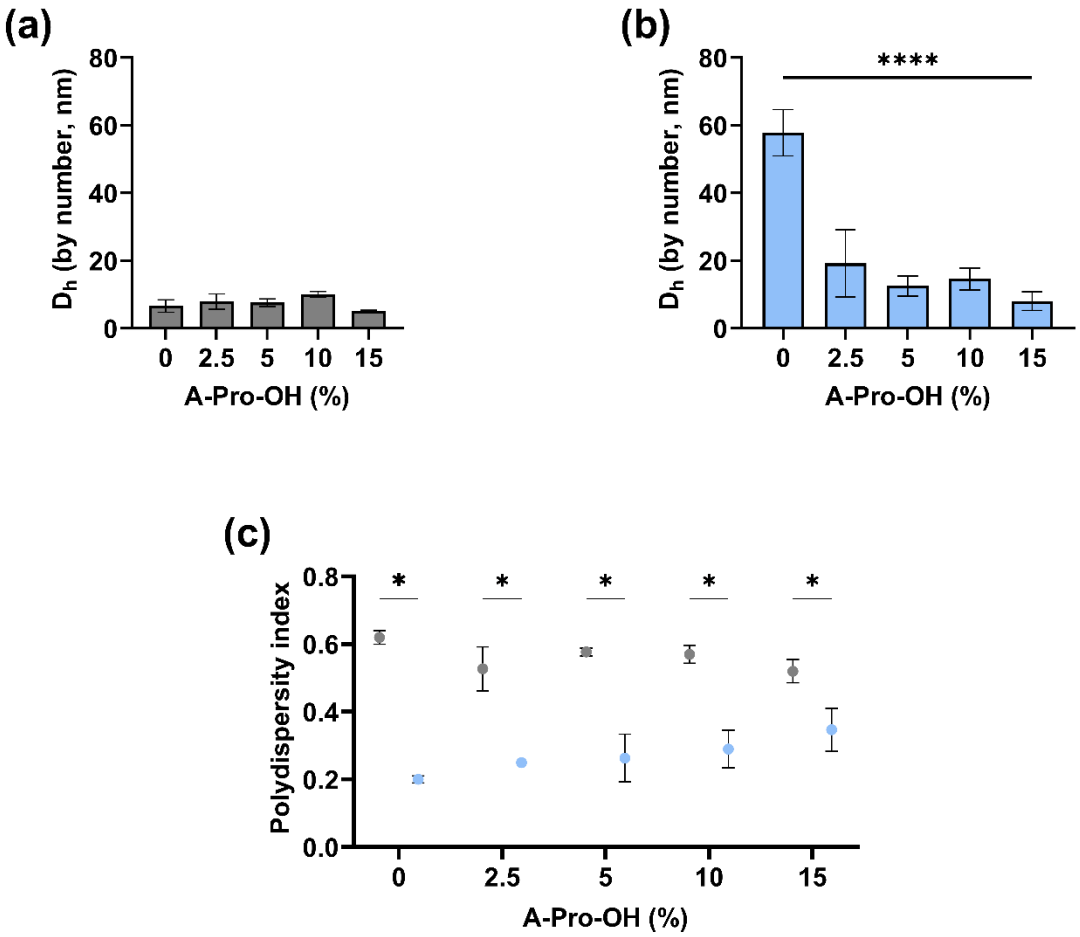

Figure 3. (a,b) Hydrodynamic diameter measured by DLS for nanogels synthesized in DMSO (a) and water (b). (c) Polydispersity index for the same formulations (water – light blue, DMSO – grey) in phosphate buffer (PB) 10 mM pH 7.4. Data are presented as mean values ± SD (n=3), **** p < 0.0001.

For the NGs synthesized in water (**Figure 3b**), the data show that the neutral NG has a much larger particle size (around 58 nm, **Figure S3**) compared to the same formulation prepared in DMSO, however when the charged monomer was introduced, the resulting polymer was considerably smaller, around 20 nm. The presence of the ionized carboxylic moiety in the A-Pro-OH monomer is likely to result in electrostatic repulsion leading to the formation of smaller particles, even when present in concentrations as low as 2.5 molar%. Interestingly, no

significant differences ($p > 0.01$) were observed for formulations with different A-Pro-OH content, suggesting that this effect is not concentration-dependent.

The analysis of the polydispersity index (PDI, **Figure 3c**) for all the preparations showed interesting results. The NGs synthesised in water had significantly lower ($p < 0.05$) PDI values than NGs synthesised in DMSO. The introduction of A-Pro-OH did not significantly ($p < 0.01$) impact the PDI values of both DMSO and water NGs for all concentrations tested. The data provide evidence that helps to interpret the solvent effect on the chemical yields. The higher PDI values in DMSO suggest that the polymerization results in a much higher proportion of smaller particles, that are then lost during the purification step by dialysis. High polydispersity has been shown to lead to a loss of colloidal stability when the NG synthesis is scaled-up[51] which provides an additional advantage, to the choice of using water as a better solvent system.

The ζ-potential values of all formulations were measured by DLS (**Figure 4**) to provide further data on the physico-chemical properties of the polymers. NGs with 2.5 molar% of A-Pro-OH showed similar ζ-potential values (around -15 mV), regardless of the solvent used during synthesis. On the other hand, water NGs with 15 molar% of A-Pro-OH showed significantly ($p < 0.001$) different surface charges (~ -30 mV) compared to DMSO (-25 mV). Interestingly, the NGs produced in water showed a direct correlation between the A-Pro-OH content and total surface charge, which cannot be observed for the NGs prepared in DMSO.

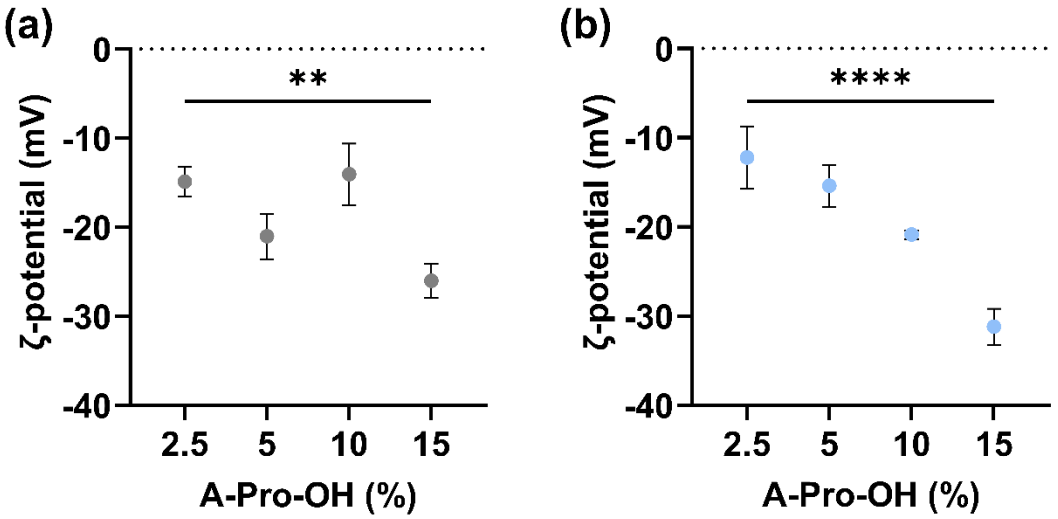

Figure 4. (a,b) ζ-Potential of different formulation in water (a) and in DMSO (b) measured in PB 10 mM pH 7.4. Data are presented as mean values ± SD (n=3), ** p < 0.05, ***p < 0.005, **** p < 0.0005.

The data obtained with DLS and ^{1}H-NMR together with the ζ-potential values provide evidence of the impact that the solvent used during the polymerization has on the morphology and properties of the NGs. When prepared in water, the ionized A-Pro-OH monomer is more likely to be localized near the surface of the NG, where it can minimize the electrostatic repulsion. The use of the KPS/TEMED pair for the initiation leads to the presence of tertiary amines end-groups in the NG network[52], potentially impacting the surface charge quantification, however no significant evidence of this was found in this case, even at low concentrations of A-Pro-OH. When prepared in DMSO, the localization of the monomers in the NG structure is influenced by their reactivity, with both A-Pro-OH and MBA having a similar and faster reactivity compared to AAm[49,53,54], resulting in a more peripheric incorporation of Aam in the particle structure. This is further confirmed by the lack of trend in ζ-potential values with increasing A-Pro-OH content for the NGs prepared in DMSO.

3.4 Transmission electron microscopy

The images obtained via transmission electron microscopy (TEM) reinforced the results obtained by DLS on the size of the particles and the effect of the introduction of the A-Pro-OH monomer in water. Overall, the introduction of the negatively charged monomer reduced the average diameter of the NGs (**Figure 5**).

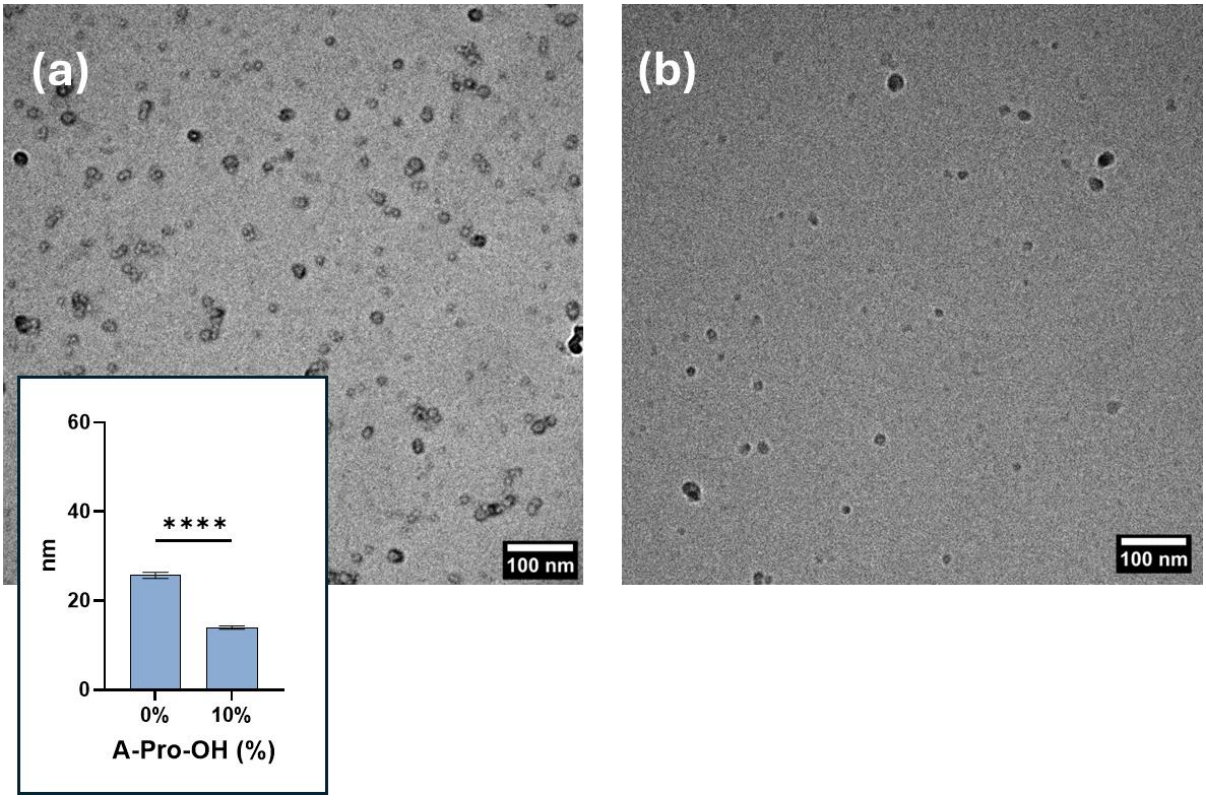

Figure 5. (a,b) Cryo-EM images of nanogels synthesised in water with no functional monomer (a) and 10% A-Pro-OH (b). Data are presented as mean values ± SEM (n = 105, **** p < 0.0001).

The size measured by cryogenic transmission electron microscopy is consistent with what observed by DLS, although the diameters observed are smaller. This is explained by the intrinsic DLS being a technique based on scattering, which provides the hydrodynamic diameter of the particles measured, as opposed to electron microscopy that provides a direct result on the particle diameter. A similar reduction in size is shown by negative staining TEM (**Figure S5**), for nanogels produced in DMSO, which contrasts with DLS results. In this case,

one of the possible explanations is that the introduction of A-Pro-OH counteracts the loss of tri-dimensional structure due to the drying effect.

Overall, the TEM data indicate that negatively charged NGs containing A-Pro-OH show different properties when synthesized in water rather than DMSO. HDRP in water leads to a better control over particle size and surface charge, as well as lower polydispersity, regardless of the amount of functional monomer introduced. These results highlight how the HDRP process can be tailored to a more sustainable, scalable and controllable approach. Further, it can support the development of negatively charged nanogels for a variety of applications, including drug delivery.

3.5 Acute cytotoxicity assay

Biocompatibility is paramount when developing new materials for drug delivery applications. Therefore, it is important to test the cytotoxicity of the NGs and evaluate if the choice of synthetic solvent, and changes in morphology and properties have any impact on how these nanoparticles interact with bioentities. For this study, we evaluated the cytotoxicity of the NGs containing up to 10 molar% of A-Pro-OH on the SH-SY5Y human neuroblastoma cell line via an MTT assay, as it is a standard and reproducible cell line[55], to evaluate a potential application of the NGs to drug delivery in cellular systems. Cells were incubated with 0.1, 0.5 mg/mL (**Figure S4**, ESI) and 1 mg/mL (**Figure 6**) of NGs synthesised in DMSO or in water. Overall, the data show that all the formulations proved to be non-toxic even at high concentrations, regardless of the A-Pro-OH content or the synthetic solvent used. The data suggest that purification steps were effective in both synthetic methods, and that the morphological differences introduced by the different solvents do not play a significant role on the biocompatibility *in vitro*. These data are coherent with reports on other cell lines regarding negatively charged NGs[27,56], and pave the way for further studies *in vivo*.

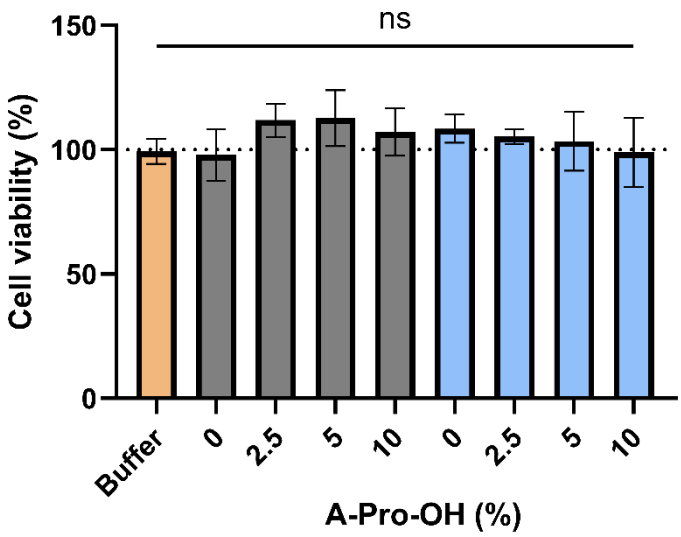

Figure 6. Cell viability expressed as percentage of medium control for different nanogels containing 0% to 10 molar% A-Pro-OH (vehicle control in orange, DMSO in grey, water in light blue). Concentration 1 mg/mL. Data are presented as mean ± SD (n=3). The changes in cell viabiliry are not statistically significant under any of the conditions tested.

4. Conclusions

This study evaluated a greener and sustainable synthetic approach for the synthesis in water of neutral and negatively charged Aam-based NGs via HDRP, without the use of surfactants, and how the change in solvent impacted the morphology and properties of the nanoparticles. The data provide evidence that water-based synthesis leads to NGs with higher monomer conversions and chemical yields, resulting in very good consistency between formulation and final composition after isolation of the NGs. The polymerization in water led to larger particle size for the neutral NG. The introduction of the A-Pro-OH monomer resulted in a smaller diameter due to the electrostatic repulsion with the growing polymer chains, confirmed both by scattering and electronic microscopy techniques;it also significantly reduced the polydispersity of the colloidal solutions. This translates into a more efficient synthetic methodology, with reduced loss of starting materials, higher potential for scalability, and reduction in costs. In addition, cytotoxicity studies were carried out on the NGs, that

demonstrated no significant reduction in viability on a human neuroblastoma cell line, supporting the suitability of these materials for biomedical applications.

Future applications of nanomaterials as drug delivery systems will be significantly impacted by the ability to develop scalable synthetic approaches. In this context, the removal of organic solvents will be key in obtaining green and sustainable methodologies. The results that we reported demonstrate that water can be utilized successfully as solvent for the synthesis of negatively charged NGs without the use of surfactants, consistently leading to particles with low polydispersity, tailored surface charge, and small particle size.

Author Contributions

D.M., G.R.: conceptualization, methodology, investigation, visualization, and writing — original draft preparation. A.R., V.R.C.: methodology, investigation, visualization and writing — reviewing and editing. M.V: writing — review and editing, supervision, and funding acquisition., M.R.: conceptualization, writing — review and editing, supervision, and funding acquisition. All authors have read and agreed to the published version of the manuscript. The authors would like to thank Marjolaine Thomas and Hui Zhang for their help in acquiring electron microscopy images.

Funding

This project has received funding from the European Union's Horizon 2020 research and innovation program under the Marie Skłodowska-Curie grant agreement No 956977 (DM, GR, AR, VRC).

Notes

The authors declare no competing financial interest.

References

1 Peer, D. *et al.* Nanocarriers as an emerging platform for cancer therapy. *Nature Nanotechnology* **2**, 751-760, doi:10.1038/nnano.2007.387 (2007).

2 Harish, V. *et al.* Review on Nanoparticles and Nanostructured Materials: Bioimaging, Biosensing, Drug Delivery, Tissue Engineering, Antimicrobial, and Agro-Food Applications. *Nanomaterials* **12**, 457, doi:10.3390/nano12030457 (2022).

3 Barhoum, A. *et al.* Review on Natural, Incidental, Bioinspired, and Engineered Nanomaterials: History, Definitions, Classifications, Synthesis, Properties, Market, Toxicities, Risks, and Regulations. *Nanomaterials* **12**, 177, doi:10.3390/nano12020177 (2022).

4 Bhadra, D., Bhadra, S., Jain, S. & Jain, N. K. A PEGylated dendritic nanoparticulate carrier of fluorouracil. *International Journal of Pharmaceutics* **257**, 111-124, doi:https://doi.org/10.1016/S0378-5173(03)00132-7 (2003).

5 Slowing, I. I., Vivero-Escoto, J. L., Wu, C.-W. & Lin, V. S. Y. Mesoporous silica nanoparticles as controlled release drug delivery and gene transfection carriers. *Advanced Drug Delivery Reviews* **60**, 1278-1288, doi:https://doi.org/10.1016/j.addr.2008.03.012 (2008).

6 Barua, S. & Mitragotri, S. Challenges associated with penetration of nanoparticles across cell and tissue barriers: A review of current status and future prospects. *Nano Today* **9**, 223-243, doi:10.1016/j.nantod.2014.04.008 (2014).

7 Nsairat, H. *et al.* Liposomes: structure, composition, types, and clinical applications. *Heliyon* **8**, e09394, doi:10.1016/j.heliyon.2022.e09394 (2022).

8 Kumari, A., Yadav, S. K. & Yadav, S. C. Biodegradable polymeric nanoparticles based drug delivery systems. *Colloids and Surfaces B: Biointerfaces* **75**, 1-18, doi:https://doi.org/10.1016/j.colsurfb.2009.09.001 (2010).

9 Kataoka, K., Harada, A. & Nagasaki, Y. Block copolymer micelles for drug delivery: design, characterization and biological significance. *Advanced Drug Delivery Reviews* **47**, 113-131, doi:https://doi.org/10.1016/S0169-409X(00)00124-1 (2001).

10 Yin, Y. *et al.* Nanogel: A Versatile Nano-Delivery System for Biomedical Applications. *Pharmaceutics* **12**, 290, doi:10.3390/pharmaceutics12030290 (2020).

11 Wang, H. *et al.* Responsive polymer–fluorescent carbon nanoparticle hybrid nanogels for optical temperature sensing, near-infrared light-responsive drug release, and tumor cell imaging. *Nanoscale* **6**, 7443-7452, doi:10.1039/c4nr01030b (2014).

12 Bhattacharya, K. *et al.* REDOX Responsive Fluorescence Active Glycopolymer Based Nanogel: A Potential Material for Targeted Anticancer Drug Delivery. *ACS Appl. Bio Mater.* **2**, 2587-2599, doi:10.1021/acsabm.9b00267 (2019).

13 Sang, G., Bardajee, G. R., Mirshokraie, A. & Didehban, K. A thermo/pH/magnetic-responsive nanogel based on sodium alginate by modifying magnetic graphene oxide: Preparation, characterization, and drug delivery. *Iranian Polymer Journal* **27**, 137-144, doi:10.1007/s13726-017-0592-3 (2018).

14 Hu, J.-C. *et al.* A ROS-Sensitive Diselenide-Crosslinked Polymeric Nanogel for NIR Controlled Release. *Chinese Journal of Polymer Science* **41**, 386-393, doi:10.1007/s10118-022-2867-1 (2023).

15 Mohammad Gholiha, H., Ehsani, M., Saeidi, A. & Ghadami, A. Albumin-loaded thermo/pH dual-responsive nanogels based on sodium alginate and poly (N-vinyl caprolactam). *Progress in Biomaterials* **12**, 41-49, doi:10.1007/s40204-022-00211-9 (2023).

16 Li, W. X. *et al.* A nanogel sensor for colorimetric fluorescence measurement of ionizing radiation doses. *Chemical Communications* **55**, 9614-9617, doi:10.1039/c9cc03680f (2019).

17 Peng, H.-S., Stolwijk, J. A., Sun, L.-N., Wegener, J. & Wolfbeis, O. S. A Nanogel for Ratiometric Fluorescent Sensing of Intracellular pH Values. *Angewandte Chemie International Edition* **49**, 4246-4249, doi:10.1002/anie.200906926 (2010).

18 Sharma, B. & Striegler, S. Nanogel Catalysts for the Hydrolysis of Underivatized Disaccharides Identified by a Fast Screening Assay. *ACS Catalysis* **13**, 1614-1620, doi:10.1021/acscatal.2c05575 (2023).

19 Pourjavadi, A., Nazari-Chamazkoti, M. & Hosseini, S. H. Polymeric ionic liquid nanogel-anchored tungstate anions: a robust catalytic system for oxidation of sulfides to sulfoxides. *New J. Chem.* **39**, 1348-1354, doi:10.1039/c4nj01931h (2015).

20 Sanson, N. & Rieger, J. Synthesis of nanogels/microgels by conventional and controlled radical crosslinking copolymerization. *Polymer Chemistry* **1**, 965, doi:10.1039/c0py00010h (2010).

21 Perrier, S. 50th Anniversary Perspective: RAFT Polymerization—A User Guide. *Macromolecules* **50**, 7433-7447, doi:10.1021/acs.macromol.7b00767 (2017).

22 Oh, J. K., Bencherif, S. A. & Matyjaszewski, K. Atom transfer radical polymerization in inverse miniemulsion: A versatile route toward preparation and functionalization of microgels/nanogels for targeted drug delivery applications. *Polymer* **50**, 4407-4423, doi:https://doi.org/10.1016/j.polymer.2009.06.045 (2009).

23 Delaittre, G., Save, M. & Charleux, B. Nitroxide-Mediated Aqueous Dispersion Polymerization: From Water-Soluble Macroalkoxyamine to Thermosensitive Nanogels. *Macromolecular Rapid Communications* **28**, 1528-1533, doi:https://doi.org/10.1002/marc.200700230 (2007).

24 Furuncuoğlu, T., Uğur, İ., Değirmenci, İ. & Aviyente, V. Role of Chain Transfer Agents in Free Radical Polymerization Kinetics. *Macromolecules* **43**, 1823-1835, doi:10.1021/ma902803p (2010).

25 Su, H. Y. *et al.* Synthesis and characterization of magnetic dextran nanogel doped with iron oxide nanoparticles as magnetic resonance imaging probe. *International Journal of Biological Macromolecules* **128**, 768-774, doi:10.1016/j.ijbiomac.2019.01.219 (2019).

26 Kim, J. *et al.* Skin penetration-inducing gelatin methacryloyl nanogels for transdermal macromolecule delivery. *Macromol. Res.* **24**, 1115-1125, doi:10.1007/s13233-016-4147-9 (2016).

27 Sarika, P. R., Anil Kumar, P. R., Raj, D. K. & James, N. R. Nanogels based on alginic aldehyde and gelatin by inverse miniemulsion technique: synthesis and characterization. *Carbohydr Polym* **119**, 118-125, doi:10.1016/j.carbpol.2014.11.037 (2015).

28 Shoyama, K. *et al.* Poly(N-isopropylacrylamide) copolymer nanogels with thermogelling ability prepared by a single step of dispersion polymerization. *Advanced Powder Technology* **33**, 103553, doi:https://doi.org/10.1016/j.apt.2022.103553 (2022).

29 Ekkelenkamp, A. E., Jansman, M. M. T., Roelofs, K., Engbersen, J. F. J. & Paulusse, J. M. J. Surfactant-free preparation of highly stable zwitterionic poly(amido amine) nanogels with minimal cytotoxicity. *Acta Biomaterialia* **30**, 126-134, doi:10.1016/j.actbio.2015.10.037 (2016).

30 Graham, N. B. & Cameron, A. Nanogels and microgels: The new polymeric materials playground. *Pure and Applied Chemistry* **70**, 1271-1275, doi:doi:10.1351/pac199870061271 (1998).

31 Maddock, S. C., Pasetto, P. & Resmini, M. Novel imprinted soluble microgels with hydrolytic catalytic activityElectronic supplementary information (ESI) available: Fig. S1 and S2: raw and corrected kinetic data of Pol396 and Pol397 with substrate. General methodology for polymer preparation and k. *Chemical Communications*, 536, doi:10.1039/b312631e (2004).

32 Anastasiadi, R.-M., Traldi, F. & Resmini, M. Imidazole-Based Monomer as Functional Unit for the Specific Detection of Paraxanthine in Aqueous Environments. *Chemosensors* **10**, 301, doi:10.3390/chemosensors10080301 (2022).

33 Papadimitriou, S. A. *et al.* Fluorescent polymeric nanovehicles for neural stem cell modulation. *Nanoscale* **8**, 17340-17349, doi:10.1039/c6nr06440j (2016).

34 Traldi, F. *et al.* Protein-Nanoparticle Interactions Govern the Interfacial Behavior of Polymeric Nanogels: Study of Protein Corona Formation at the Air/Water Interface. *International Journal of Molecular Sciences* **24**, 2810, doi:10.3390/ijms24032810 (2023).

35 Vdovchenko, A., Pearce, A. K., Freeley, M., O'Reilly, R. K. & Resmini, M. Effect of heterogeneous and homogeneous polymerisation on the structure of pNIPAm nanogels. *Polymer Chemistry* **12**, 6854-6864, doi:10.1039/d1py01333e (2021).

36 Serrano-Medina, A., Cornejo-Bravo, J. M. & Licea-Claveríe, A. Synthesis of pH and temperature sensitive, core–shell nano/microgels, by one pot, soap-free emulsion polymerization. *J. Colloid Interface Sci.* **369**, 82-90, doi:https://doi.org/10.1016/j.jcis.2011.12.045 (2012).

37 Alvarado Mendoza, A. G., Zárate-Navarro, M. A., Ceja, I. & Cortés-Ortega, J. A. The effect of water/ethanol ratio and monomer concentration on the size and morphology of polyacrylamide nanogels in a surfactant-free synthesis. *Journal of Macromolecular Science, Part A* **57**, 91-97, doi:10.1080/10601325.2019.1671772 (2020).

38 Rana, M. M., Natale, G. & De la Hoz Siegler, H. A greener route for smart PNIPAm microgel synthesis using a bio-based synthesis-solvent. *European Polymer Journal* **174**, 111311, doi:https://doi.org/10.1016/j.eurpolymj.2022.111311 (2022).

39 El-Halah, A., González, N., Contreras, J. & López-Carrasquero, F. Effect of the synthesis solvent in swelling ability of polyacrylamide hydrogels. *Journal of Polymer Research* **27**, doi:10.1007/s10965-019-1988-x (2020).

40 Huang, Y.-C., Zeng, Y.-J., Lin, Y.-W., Tai, H.-C. & Don, T.-M. In Situ Encapsulation of Camptothecin by Self-Assembly of Poly(acrylic acid)-b-Poly(N-Isopropylacrylamide) and Chitosan for Controlled Drug Delivery. *Polymers* **15**, 2463, doi:10.3390/polym15112463 (2023).

41 Jorge, A. R., Chernobryva, M., Rigby, S. E. J., Watkinson, M. & Resmini, M. Incorporation of Cobalt-Cyclen Complexes into Templated Nanogels Results in Enhanced Activity. *Chemistry - A European Journal* **22**, 3764-3774, doi:10.1002/chem.201503946 (2016).

42 Judah, H. L., Liu, P., Zarbakhsh, A. & Resmini, M. Influence of Buffers, Ionic Strength, and pH on the Volume Phase Transition Behavior of Acrylamide-Based Nanogels. *Polymers* **12**, 2590, doi:10.3390/polym12112590 (2020).

43 Mudassir, J., Darwis, Y. & Yusof, S. R. Synthesis, characterization and toxicological evaluation of pH-sensitive polyelectrolyte Nanogels. *Journal of Polymer Research* **24**, 164, doi:10.1007/s10965-017-1321-5 (2017).

44 Salinas, Y., Castilla, A. M. & Resmini, M. An <scp>l</scp>-proline based thermoresponsive and pH-switchable nanogel as a drug delivery vehicle. *Polymer Chemistry* **9**, 2271-2280, doi:10.1039/c8py00308d (2018).

45 Li, Y. J. *et al.* Solubility in Different Solvents, Crystal Polymorph and Morphology, and Optimization of Crystallization Process of AIBN. *Journal of Chemical & Engineering Data* **63**, 27-38, doi:10.1021/acs.jced.7b00538 (2018).

46 Pascal, P., Napper, D. H., Gilbert, R. G., Piton, M. C. & Winnik, M. A. Pulsed laser study of the propagation kinetics of acrylamide and methacrylamide in water. *Macromolecules* **23**, 5161-5163, doi:10.1021/ma00226a024 (1990).

47 Coote, M. L., Davis, T. P., Klumperman, B. & Monteiro, M. J. A Mechanistic Perspective on Solvent Effects in Free-Radical Copolymerization. *Journal of Macromolecular Science, Part C: Polymer Reviews* **38**, 567-593, doi:10.1080/15583729808546032 (1998).

48 Kurenkov, V. F. & Abramova, L. I. Homogeneous Polymerization of Acrylamide in Solutions. *Polymer-Plastics Technology and Engineering* **31**, 659-704, doi:10.1080/03602559208017774 (1992).

49 Liu, P., Pearce, C. M., Anastasiadi, R.-M., Resmini, M. & Castilla, A. M. Covalently Crosslinked Nanogels: An NMR Study of the Effect of Monomer Reactivity on Composition and Structure. *Polymers* **11**, 353, doi:10.3390/polym11020353 (2019).

50 Bilardo, R., Traldi, F., Brennan, C. H. & Resmini, M. The Role of Crosslinker Content of Positively Charged NIPAM Nanogels on the In Vivo Toxicity in Zebrafish. *Pharmaceutics* **15**, 1900, doi:10.3390/pharmaceutics15071900 (2023).

51 Simpson, M. J., Corbett, B., Arezina, A. & Hoare, T. Narrowly Dispersed, Degradable, and Scalable Poly(oligoethylene glycol methacrylate)-Based Nanogels via Thermal Self-Assembly. *Industrial & Engineering Chemistry Research* **57**, 7495-7506, doi:10.1021/acs.iecr.8b00793 (2018).

52 De Feng, X. Q., Xin Guo; Qiu, Kun Yuan. Study of the initiation mechanism of the vinyl polymerization with the system persulfate/N,N,N′,N′-tetramethylethylenediamine. *Die Makromolekulare Chemie* **189**, 77-83, doi: https://doi.org/10.1002/macp.1988.021890108 (1988).

53 Stieger, M., Richtering, W., Pedersen, J. S. & Lindner, P. Small-angle neutron scattering study of structural changes in temperature sensitive microgel colloids. *JOURNAL OF CHEMICAL PHYSICS* **120**, 6197-6206, doi:10.1063/1.1665752 (2004).

54 Berndt, I., Pedersen, J. S. & Richtering, W. Structure of Multiresponsive "Intelligent" Core–Shell Microgels. *Journal of the American Chemical Society* **127**, 9372-9373, doi:10.1021/ja051825h (2005).

55 Dubey, S. K. *et al.* Recent Expansions on Cellular Models to Uncover the Scientific Barriers Towards Drug Development for Alzheimer's Disease. *Cellular and Molecular Neurobiology* **39**, 181-209, doi:10.1007/s10571-019-00653-z (2019).

56 Mudassir, J., Darwis, Y. & Yusof, S. R. Synthesis, characterization and toxicological evaluation of pH-sensitive polyelectrolyte Nanogels. *Journal of Polymer Research* **24**, doi:10.1007/s10965-017-1321-5 (2017).